

# Electrostatic Potential Maps and Natural Bond Orbital Analysis: Visualization and Conceptualization of Reactivity in Sanger's Reagent

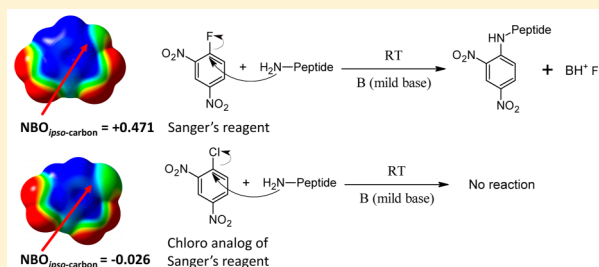
Jeffery D. Mottishaw, Adam R. Erck, Jordan H. Kramer, Haoran Sun,\* and Miles Koppang\*

Department of Chemistry, University of South Dakota, Vermillion, South Dakota 57069, United States

**S** Supporting Information

**ABSTRACT:** Frederick Sanger's early work on protein sequencing through the use of colorimetric labeling combined with liquid chromatography involves an important nucleophilic aromatic substitution ( $S_NAr$ ) reaction in which the N-terminus of a protein is tagged with Sanger's reagent. Understanding the inherent differences between this  $S_NAr$  reaction and other nucleophilic substitution reactions ( $S_N1$  and  $S_N2$ ) can be challenging for students learning organic chemistry. Here, both electrostatic potential (ESP) maps and natural bond orbital (NBO) analyses are employed to visualize and conceptualize Sanger's key observation of the difference in reactivity between 2,4-dinitrochlorobenzene and 2,4-dinitrofluorobenzene. The utility of this method is extended to compare the reactivity of a series of halobenzenes for  $S_NAr$  fluorination, a widely used reaction in pharmaceutical and medicinal fields. In combination with experimental results from the literature, the ESP maps and NBO analyses are consistent with and provide excellent corroboration with the reactivity of different substrates toward  $S_NAr$  reactions.

**KEYWORDS:** Organic Chemistry, Molecular Modeling, Second-Year Undergraduate, Graduate Education/Research, Computer-Based Learning



## INTRODUCTION

Protein and peptide analyses, both heavily-used experimental procedures in biochemistry and medicinal chemistry, possess deep roots in fundamental organic and analytical chemistries. With the development of electrospray ionization methods and reduced costs for liquid chromatography mass spectrometry (LC-MS), LC-MS has become the popular choice for amino acid, peptide, and protein analysis.<sup>1–3</sup> Before the advancements in mass spectrometry, derivatization of amino acids and peptides with chromophoric, fluorophoric, and electrophoric tags were commonly used to achieve both increased sensitivity and selectivity in the detection phase following liquid chromatographic separation. Popular derivatization reagents included 2,4-dinitrofluorobenzene (DNFB; Sanger's reagent),<sup>4</sup> phenyl isothiocyanate (Edman's reagent),<sup>5</sup> ninhydrin,<sup>6</sup> dabsyl chloride,<sup>7</sup> fluorescamine,<sup>8</sup> dansyl chloride,<sup>9</sup> and *o*-phthalaldehyde (OPA).<sup>10</sup>

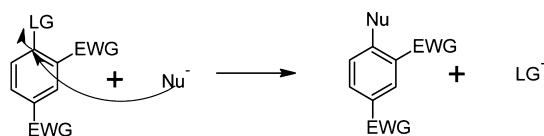
Sanger's reagent is especially noteworthy for its role in the structure elucidation of insulin, which resulted in the first of two Nobel Prizes in Chemistry for Frederick Sanger.<sup>11</sup> The chemistry of Sanger's reagent can be found in undergraduate organic textbooks ranging from classical<sup>12</sup> to modern texts.<sup>13</sup> Sanger's elucidation of the structure of insulin<sup>14</sup> is also discussed in biochemistry textbooks, with emphasis on the landmark discovery that proteins have distinct amino acid sequences.<sup>15</sup> The fundamental chemistry of Sanger's reagent, nucleophilic aromatic substitution ( $S_NAr$ ),<sup>16</sup> has been discussed

in many organic texts<sup>17</sup> as part of an organic chemistry curriculum. However, students often encounter some levels of difficulty in understanding the reactivity of Sanger's reagent compared to other derivatives with similar composition and structure. One example of this is in the difference in reactivity between 2,4-dinitrochlorobenzene (DNFB) and DNFB toward  $S_NAr$ . An easy-to-use and convincing pedagogical approach is necessary for teaching this interesting, yet challenging,  $S_NAr$  chemistry.

Sanger's reagent bridges many important biological, pharmaceutical, and medicinal applications through the fundamentally important  $S_NAr$  reaction mechanism in organic chemistry. Understanding the reactivity of Sanger's reagent and its derivatives toward  $S_NAr$  reaction is an exciting starting point for many students to learn mechanistic organic chemistry and how it applies to the medical field. Though pedagogical tools for electrophilic aromatic substitution have been mentioned in the literature,<sup>18–24</sup> ways to help students understand  $S_NAr$  reactions have received considerably less attention.<sup>25–28</sup> In contrast to other aromatic substitution reactions, such as electrophilic aromatic substitution (e.g., Friedel-Crafts acylation),  $S_NAr$  requires a highly electron-deficient reaction center, which is often the *ipso* carbon, that is directly connected to the leaving group. The rate-determining step of the  $S_NAr$  reaction is

the attack of a nucleophile onto an electrophilic aromatic carbon directly connected to the leaving group which is normally a halogen or a nitro group (Scheme 1).

### Scheme 1. Mechanism of $S_NAr$ Reaction<sup>a</sup>



<sup>a</sup>EWG = electron-withdrawing group, LG = leaving group, Nu = nucleophile.

The  $S_NAr$  reaction is strongly influenced by the electron density at the *ipso* carbon. Strong electron-withdrawing substituents, such as nitro groups, attached at the *ortho* and *para* positions to the *ipso* carbon will greatly reduce the electron density on the *ipso* carbon and will activate it to the nucleophilic attack. Though the leaving group is not directly involved in the rate-determining step of the reaction, it does affect the electron density of the *ipso* carbon at the reaction center. Because bimolecular reactions require a strong pairing of a nucleophile and an electrophile,<sup>17</sup> it is important to maximize the charge difference between these two elements of the reaction. To assist students to understand these fundamental principles associated with  $S_NAr$  reactions, electrostatic potential (ESP) maps<sup>29</sup> and natural bond orbital (NBO)<sup>30</sup> analysis were used to visualize and conceptualize the reactivity of Sanger's reagent and the reactivity difference between Sanger's reagent and its analogues toward  $S_NAr$  reactions. On the basis of the latter results, a generalized pedagogical approach into  $S_NAr$  reactions is described based on nucleophilic aromatic fluorination.

ESP<sup>29</sup> and NBO<sup>30</sup> calculations, used for a number of years as a guide in synthesis and chemical reactivity, have gained increased usage in recent years to augment chemical education.<sup>31–36</sup> For example, NBO analysis was used to understand the results from an iodochlorination of alkenes in the undergraduate chemistry laboratory,<sup>37</sup> and to clarify basic structural concepts in both graduate and undergraduate organic courses.<sup>38</sup> Recently, the use of ESP maps was surveyed in 45 general and organic chemistry textbooks.<sup>39</sup> Although questions continue to be raised regarding the effectiveness of ESP maps for chemical understanding, the use of computational methods has increased dramatically in the chemical education arena. The presence of ESP maps in chemistry textbooks at the undergraduate level is becoming ubiquitous, and it is important for students to understand how theory and experiment are correlated through computational technology.

With the passing of Frederick Sanger in November 2013, we also wished to present the ESP and NBO analysis results on the  $S_NAr$  reaction of 2,4-dinitrofluorobenzene in honor of his life and creative work, emphasizing his seminal work with DNFB. These analyses also demonstrate to undergraduate students the power of fundamental concepts and principles in real world applications. This demonstration is also expected to encourage students to learn the important fundamental concepts and principles of mechanistic exploration through computational methods that could assist them in their preparation to become future problem solvers.

## COMPUTATIONAL METHODS

### Electrostatic Potential (ESP) Maps

Density Functional Theory<sup>40</sup> (DFT) with the B3LYP and 6-31g(d) functional/basis set combination<sup>41</sup> was used to generate all images. Gaussian 09<sup>42</sup> was used for the numerical data derived from a quantum mechanical analysis, and GaussView<sup>43</sup> was used to process the data and generate ESP maps. Each ESP map (unless otherwise specified) used consistent isovalues and color scaling for related compounds. A typical calculation was ran on four processors and completed within an hour.

### Natural Bond Orbital (NBO) Analysis

Full NBO population analyses were done with Gaussian 09 and GaussView software at the B3LYP/6-31g(d) level of theory, and were performed at the same time as the initial geometry optimization and subsequent generation of ESP data (see Supporting Information for example input files).

## RESULTS AND DISCUSSION

### 1. ESP Maps

To make comparisons between different substituents on the same carbon atom using ESPs, it is crucial to use the same methodology to generate them, and then to use the same visual parameters to generate the images. The DFT method with 6-31g(d) functional/basis set combination provides an excellent description of ground state organic compounds within a reasonable amount of CPU time. Calculation of many small organic molecules (for example, molecules shown in Figure 1)

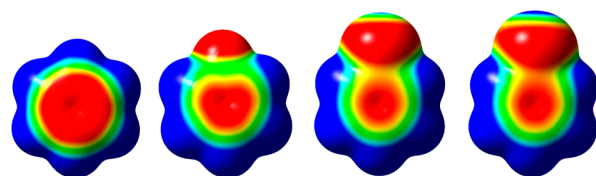


**Figure 1.** ESP maps (left to right) of benzene, fluorobenzene, chlorobenzene, and bromobenzene. All maps used consistent surface potential ranges (−0.015000 au (red) to 0.000010 au (blue)) and an isovalue of 0.000400 au. Here, isovalue is the cutoff electron density from the molecular calculations used to define the outer boundary of the molecule.

can be done within a few minutes to an hour on a laptop computer with i-7 CPU and 16 GB RAM, making these types of calculations relatively accessible to instructors. Many other computational programs, including the free GAMESS-US program,<sup>44</sup> coupled with a graphics program such as MacMolPlt,<sup>45</sup> can accomplish the same goal with no associated software purchase. These can also be performed on desktop or laptop computers running any operating system, making them potentially accessible to a wide range of instructors.

An ESP map is a representation where the electrostatic potential at the molecular surface is indicated by colors. ESP maps allow for an easy to understand visualization of the distribution of charge in a molecule.<sup>46</sup> Typically, the color scheme selected for ESP maps designates red corresponding to regions of high electron density and blue corresponding to regions of low electron density, with yellow and green intermediate levels.<sup>47,48</sup> The color scale of electrostatic potential is typically symmetrically distributed across the surface potential range referencing a surface potential value of zero as the center of the color scale; for example, pure red color

represents a surface potential value of  $-0.01$  au and a pure blue color represents a surface potential value of  $0.01$  au. The color scale is a relative scale that assists the visualization of the charge distribution difference over the molecular surface. To emphasize the charge distribution difference among similar molecules, an unsymmetrical color scale of electrostatic potential can be distributed across the surface potential range; for example, a pure red color represents a surface potential value of  $-0.0001$  au and a pure blue color represents a surface potential value of  $0.05$  au. In the former case, a pure green color represents a surface potential value of  $0$  au; however, in the latter case, a pure green color represents a positive surface potential value of  $0.02495$  au, the midpoint between  $-0.0001$  and  $0.05$  au. ESP maps of monosubstituted halobenzenes with an unsymmetrical color scale that helps to visualize the charge difference on the *ipso* carbon and the detailed charge distribution on halogen atoms are shown in Figure 1. These maps are especially important to understand halogen bonding in crystal engineering, although this halogen bonding topic would only be appropriate for a graduate-level course.

A comparison of the ESP maps for a series of halobenzenes illustrates their value in the visualization of fundamental organic chemistry concepts. Benzene shows a larger amount of electron density in the center of the ring (indicated by the red shading), and a lower amount at the hydrogen peripheries (indicated by the blue shading). This is consistent with the large  $\pi$ -electron cloud induced by the aromatic system. Through this ESP map comparison, the concept of electron density can be connected to basic NMR principles, such as the deshielding of proton signals at specific positions on the ring.<sup>36</sup> The idea of substituents affecting electron density within the ring is illustrated by the introduction of fluorine, where there is a significant reduction in electron density in the center of the ring (as seen in size reduction of the red color region in the ring area), owing to the high electronegativity of fluorine. When compared to the ESP maps of chlorobenzene and bromobenzene, the ESP map of fluorobenzene shows a greater area of red color region in the center of the molecule than that of chlorobenzene and bromobenzene, indicating the  $\pi$ -electron density in fluorobenzene is greater than that of chlorobenzene and bromobenzene. This observation clearly demonstrates the  $\pi$ -donating property of the fluorine substituent in addition to its  $\sigma$ -withdrawing property. An additional feature is seen at the side of the halogen opposite of the ring, represented by a green band and a blue tip (for example, bromobenzene ESP map in Figure 1). This indicates lowered electron density at this part of the halogen, and can be explained and rationalized through polarization of the p-orbital of the halogen atom. This orbital polarization effect in large halides leads to halogen bonding interactions in solid state structures, yet another principle to be visualized with these ESP maps.<sup>49,50</sup> ESP maps can also be used to explain *meta* versus *para* attack of electrophilic aromatic substitution reactions.<sup>51</sup>

Although ESP maps are very useful for illustrating fundamental concepts of reactivity of organic molecules, the use of ESP maps requires careful setup of the color scale corresponding to the potential surface value to prevent a reader from drawing misleading conclusions. First, the scaling and color schemes of potential surface values are inherently subjective, although governed by a loose convention.<sup>47</sup> Color schemes and scaling values may vary from different textbooks, journal articles, or quantum chemical visualization programs,

which make ESP maps more a qualitative tool than an absolute electronic representation of a molecular electronic structure. Second, the results will be misleading if a consistent color scale for surface potential and surface isovalue of the entire series of molecules is not used, even if the same level of computational theory is used to generate all the ESP maps in the same series of molecules. To illustrate how misleading information could easily occur, the ESP maps of the halobenzene series in Figure 1 were calculated with a different color scale of surface potential for each individual molecule (Figure 2).

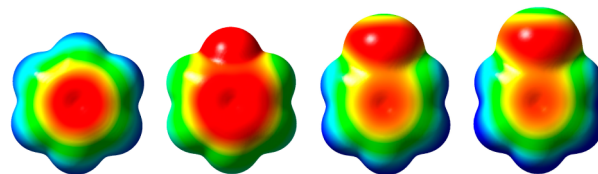


**Figure 2.** Example of misleading ESP maps caused by using inconsistent color scale of surface potential. Manipulated ESP maps (left to right) of benzene ( $-0.021000$  au (red) to  $0.015000$  au (blue)), fluorobenzene ( $-0.010000$  au (red) to  $0.030000$  au (blue)), chlorobenzene ( $-0.170000$  au to  $0.020000$  au), and bromobenzene ( $-0.017500$  au to  $0.017500$  au). Isovalue is  $0.000400$  au.

Figure 2 indicates that the fluorosubstitution increases rather than decreases the  $\pi$ -electron density of the aromatic system compared to benzene. This (misleading) result, which goes against experimental experience and chemical intuition, demonstrates the need for consistent scaling of surface potential when comparing compounds with similar structure. Furthermore, because of electronic structure differences between benzene and hexane, for example, it is not feasible to have a universal color scale to represent all surface potential ranges for all types of molecules. Instead, it is important, when illustrating substituent effects in the organic curriculum, to treat organic molecules with similar carbon cores and hybridization under the same conditions, i.e., color scale of surface potential and isovalue, as failing to do so may inadvertently confuse students.

## 2. Synergy of ESP Maps with NBO Analysis

The results obtained from a molecular orbital calculation do not represent localized bonding well; as such, other methods are needed to relate a wave function generated by quantum chemical calculations to the bonding familiar to an organic chemist.<sup>52</sup> NBO analyses are an excellent tool to relate the results of quantum chemical calculations to familiar concepts such as Lewis structures and resonance.<sup>53</sup> While there are other methods to describe electron distribution numerically and to perform population analysis, such as the Mulliken scheme,<sup>54</sup> NBO analysis offers the distinct advantages of being relatively insensitive to basis set changes,<sup>30</sup> and are often incorporated into standard quantum chemical software packages such as Gaussian or GAMESS-US. The insensitivity to the basis set used in particular calculations allows an instructor to perform quick calculations with small basis sets, and obtain quality results that can be readily compared to illustrate the desired chemical concept. Many graphical software interfaces permit the inclusion of NBO data in a relatively simple manner, and to obtain the data in tabular or graphical form with each atom labeled with its corresponding NBO value. The sum of all NBO values for each atom equals zero for a neutral molecule and the whole charge of a charged species. A negative NBO value

represents a partial negative charge, which is greater electron density or electron rich at that atom relative to other atoms; and a positive NBO value represents a partial positive charge, which is less electron density or electron poor at that atom relative to other atoms.

The strength of NBO analysis, along with the visual images of ESP maps, is that together they help to remove the subjectivity of color scheme choice by the program. Therefore, in the study of halogen substituent effects in reactions involving Sanger's reagent, a combined ESP and NBO analysis approach was used to visualize and quantify the data.

While ESP maps give qualitative visualization of relative charge distribution, NBO analyses add synergy to ESP maps by giving absolute values of partial charge located on a specific atom in a molecule. These values can then be correlated to resonance (Lewis) structures, one of the most important concepts for students to grasp in organic chemistry. NBO values calculated at the B3LYP/6-31g(d) level of theory of halobenzene series (Figure 1) are in Table 1. While the color

**Table 1. Calculated NBO Values for Monosubstituted Benzene Molecules<sup>a</sup>**

| Substituent | NBO Value of Substituent | NBO Value of <i>ipso</i> Carbon |
|-------------|--------------------------|---------------------------------|
| –H          | 0.235                    | –0.235                          |
| –F          | –0.335                   | 0.419                           |
| –Cl         | –0.010                   | –0.043                          |
| –Br         | 0.051                    | –0.109                          |

<sup>a</sup>Calculated at the B3LYP/6-31g(d) level of theory.

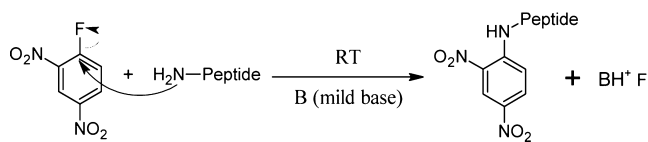
scale (red-green-blue) of ESP maps only represents the relative charge distribution of the given molecule or a series of similar molecules, it does not necessarily reflect the NBO charge value of a given atom on a molecule. In other words, one could change the color scale of ESP maps by changing the surface potential values to make the color of a particular atom or substituent more red compared to one in other molecules in the same comparison series to enhance the visualization effect.

In benzene, the hydrogen on the *ipso* carbon has partial positive charge of 0.235, while the *ipso* carbon has partial negative charge value of –0.235, which is explained by their differences in electronegativity and the inductive effects of aromaticity on the charge distribution. In fluorobenzene, the fluoro group is strongly withdrawing as indicated by a negative NBO value (–0.335), and this results in the corresponding *ipso* carbon having a positive NBO value (0.419). In chlorobenzene, the magnitude of negative charge localized on the chloro group (–0.010) is much less by an order of magnitude compared to the fluoro group in fluorobenzene, and the *ipso* carbon shows a partial negative charge (–0.043), though not to the extent of benzene. Perhaps most counterintuitive in this series is that the halide in bromobenzene is *positively* charged (0.051), and this results in an *ipso* carbon with a larger negative NBO value (–0.109) than that of chlorobenzene. ESP maps alone simply show a visual trend, but the power in combining ESP maps with NBO values is that it gives an exact reference and an explicit value on charge distribution. Coupling NBO analysis with the visual information present in ESP maps potentially permits students to make connections between chemical structure and reactivity of a reagent that either method alone would not provide.

### 3. Applications to Nucleophilic Aromatic Substitution Reactions

One application of the harmonious use of both methods is in understanding, visualizing, and conceptualizing the reactivity of Sanger's reagent. Under basic conditions, the N-terminus of a peptide (or  $\alpha$ -amino group of an amino acid) attacks the fluorinated *ipso* carbon of DNFB (Scheme 2) that results in a

**Scheme 2. Reaction of Sanger's Reagent**



chromophoric tag attached to the peptide or amino acid, allowing for spectroscopic identification of the peptide or amino acid. The nitro groups at the *ortho* and *para* positions with respect to the fluoro group serve to facilitate the nucleophilic attack on Sanger's reagent.

Sanger wrote in a key paper on the use of this reagent in the structure elucidation of insulin: "DNFB will not react with amino-acids in NaHCO<sub>3</sub> solution unless heat is applied, and this brings about a certain amount of hydrolysis of the protein. Fortunately, however, the corresponding fluoro-compound, 2,4-dinitrofluorobenzene (DNFB) was found to react readily at room temperature, and the use of this has met with considerable success..."<sup>4</sup> Here, NBO analyses and ESP maps were used to understand the reactivity difference between Sanger's reagent and its analog DNCB. Simple analyses of NBO values and ESP maps showed that, by having greater positive charge on the *ipso* carbon, the fluoro-substituted *ipso* carbon was much more reactive than that of its chloro- and bromo- analogues (Figure 3 and Table 2).

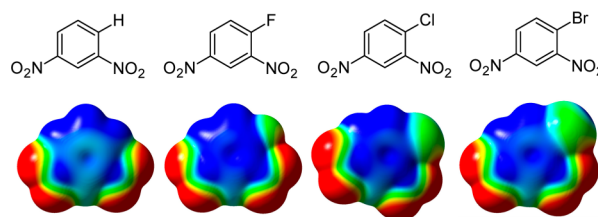


**Figure 3.** ESP maps of (left to right) 1,3-dinitrobenzene, DNFB, DNCB, and 2,4-dinitrofluorobenzene. Surface potential ranges are –0.015000 au (red) to 0.025500 au (blue). Isovalue is 0.000400 au.

The NBO values at the *ipso* position with respect to the halogen illustrates that, of the substituents in this series, only the *ipso* carbon containing a fluoro group has a positive charge. Therefore, DNFB should be much more amenable to undergo

**Table 2. Calculated NBO Values for 2,4-Dinitrosubstituted Halobenzene Molecules<sup>a</sup>**

| Substituents | NBO Value of Substituents | NBO Value of <i>ipso</i> Carbon |
|--------------|---------------------------|---------------------------------|
| –H           | 0.280                     | –0.186                          |
| –F           | –0.287                    | 0.471                           |
| –Cl          | 0.092                     | –0.026                          |
| –Br          | 0.167                     | –0.099                          |

<sup>a</sup>Calculation was done at the B3LYP/6-31g(d) level of theory.

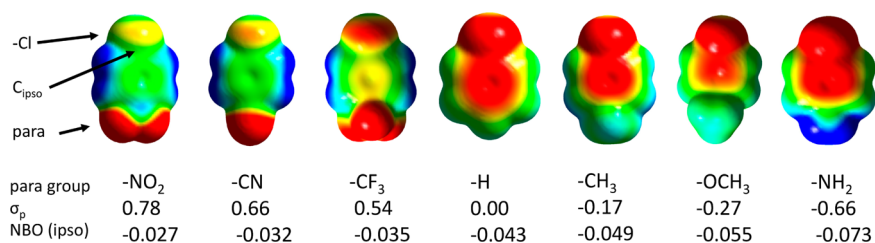
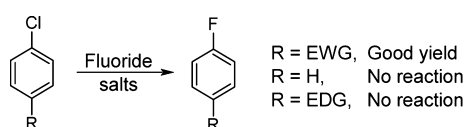


Figure 4. ESP maps and NBO values for a series of *para*-substituted chlorobenzenes.

an S<sub>N</sub>Ar reaction at room temperature, matching the experimental observations by Sanger.

The same approach was used to explain how a substituent on an aromatic substrate can affect the S<sub>N</sub>Ar reaction, in general, with nucleophilic aromatic fluorination of haloaromatics or nitroaromatics. The ESP maps and corresponding NBO analyses results for a series of *para*-substituted chlorobenzenes are shown in Figure 4. Experimental results (Scheme 3) show

### Scheme 3. Nucleophilic Aromatic Fluorination Reaction<sup>a</sup>



<sup>a</sup>EWG, electron withdrawing groups; EDG, electron donating groups

that a nucleophilic fluorination reaction only occurs for those chlorobenzenes with strong electron withdrawing substituents (e.g., CN) on the *para*-position.<sup>55,56</sup> Chlorobenzenes without electron-withdrawing substituents or with electron-donating substituents (e.g., NH<sub>2</sub>) do not undergo nucleophilic aromatic fluorination even with the most active nucleophilic fluorinating reagent, anhydrous tetrabutylammonium fluoride (TBAF<sub>anh</sub>).<sup>56</sup> The ESP maps in Figure 4 clearly show the electron density difference at the *ipso* carbon with NO<sub>2</sub>-substituted chlorobenzene displaying the least negative charge and the *ipso* carbon with NH<sub>2</sub>-substituted chlorobenzene displaying the most negative charge. The NBO values of the *ipso* carbon show the same trend as ESP maps. The calculated NBO values for *ipso* carbon also correlate linearly with the Hammett sigma para parameters with an R<sup>2</sup> value >92% for linear fitting. Since nucleophilic attack is the rate-limiting step of the S<sub>N</sub>Ar reaction, the reaction will proceed faster for those aromatic compounds with strong electron withdrawing substituents, whereas the *ipso* carbon possesses relatively lower negative, if not positive, charge.

One facet that must be stressed in examining reactivity using combined NBO and ESP analysis is that these are not true kinetic parameters, and other factors, such as stabilization of the transition state through leaving group orbital interactions, may be more relevant.<sup>57,58</sup> However, the utility in using ESP maps along with NBO values at least provide plausible explanations for experimental observations. It is also important to note that coloring on ESP maps is subjective, and NBO values are often atom-centered and cannot show all of the intricacies immediately available through a simple visual analysis of an ESP map. Therefore, a combined approach provides benefits to potentially allow students to see multiple facets of chemical reactivity at a glance.

A preliminary study was done on the effectiveness of using combined ESP maps and NBO analysis on a small number (33)

of students divided into three different sections. Two sections of students (21) were completing a full year of organic chemistry, whereas one section of students (12) had not taken organic chemistry at this time. Each student was provided information on Sanger's reagent and its use for derivatizing amino acids. They were also provided information from Sanger's original paper (vide supra) in terms of the observations of DNFB versus DNCB reactivity. Half of the students were provided additional information in the form of ESP maps and NBO values. Each student was then given four multiple choice questions regarding the reaction. Students without prior organic chemistry instruction, and who were provided the ESP maps, scored on average one question better out of four questions versus those without the ESP maps (2.9 with ESP maps out of 4 questions versus 2.3 without ESP maps on the 4 questions). The other students who had completed organic chemistry scored essentially the same whether they were provided the ESP maps or not. Interestingly, those with the ESP maps and organic chemistry experience were distracted by the ESP maps on a question regarding steric hindrance and incorrectly answered that steric hindrance, rather than electronic effects, was the reason for differences in kinetics between DNFB and DNCB.

The effectiveness test on teaching students organic chemistry using this combined ESP maps and NBO analysis method requires a systematic approach with student numbers in lecture sections large enough for good statistical analysis. The number of students and sections involved in our test was too small to properly assess the value of using ESP maps and NBO analysis. Further assessment of this combined teaching method is needed to reach reliable measurements on the method's effectiveness.

## CONCLUSION

Through an analysis of the reactivity of Sanger's reagent toward S<sub>N</sub>Ar reaction and the reactivity difference between Sanger's reagent and its analogue 2,4-dinitrochlorobenzene, the usefulness of a combined ESP maps and NBO analyses in teaching S<sub>N</sub>Ar reaction was successfully demonstrated. Further discussion on nucleophilic aromatic fluorination reaction shows a broader impact of this combined computational approach in organic chemistry teaching. The importance of using consistent color scheming when referencing ESP maps of a series of similar molecules was also demonstrated. Modern computer hardware, freely available quantum chemical calculation software, and visualization software together made possible that such approach can be done on instructors' own desktops or laptop computers within minutes. Using NBO analyses, along with the very ESP map representations, demonstrates a powerful, yet very practical approach to teaching fundamental organic chemistry.

## ■ ASSOCIATED CONTENT

### ■ Supporting Information

The Supporting Information is available on the ACS Publications website at DOI: [10.1021/ed5006344](https://doi.org/10.1021/ed5006344).

Detailed computational methods; coordinates for optimized geometries for all computed compounds (PDF, DOCX)

## ■ AUTHOR INFORMATION

### Corresponding Authors

\*E-mail (H.S.): [Haoran.Sun@usd.edu](mailto:Haoran.Sun@usd.edu).

\*E-mail (M.K.): [Miles.Koppang@usd.edu](mailto:Miles.Koppang@usd.edu).

### Notes

The authors declare no competing financial interest.

## ■ ACKNOWLEDGMENTS

H.S. thanks the NSF (CAREER, Award No. CHE-1355677) and the Center for Teaching and Learning (Teaching improvement grant) at the University of South Dakota for financial support. H.S. and M.K. acknowledge NSF REU program (Award No. CHE-1063000 and CHE-1460872). J.D.M. thanks the NSF IGERT program (Award No. DGE-0903685) for support of his graduate study. Authors also acknowledge the University of South Dakota high performance computing facility and Douglas Jennewein for IT support with the cluster computer.

## ■ REFERENCES

- (1) Kaspar, H.; Dettmer, K.; Chan, Q.; Daniels, S.; Nimkar, S.; Daviglus, M. L.; Stampler, J.; Elliott, P.; Oefner, P. J. Urinary amino acid analysis: A comparison of iTRAQ-LC-MS/MS, GC-MS, and amino acid analyzer. *J. Chromatogr. B: Anal. Technol. Biomed. Life Sci.* **2009**, *877* (20–21), 1838–1846.
- (2) Wolters, D. A.; Washburn, M. P.; Yates, J. R., III An automated multidimensional protein identification technology for shotgun proteomics. *Anal. Chem.* **2001**, *73* (23), 5683–5690.
- (3) Greenbaum, D.; Colangelo, C.; Williams, K.; Gerstein, M. Comparing protein abundance and mRNA expression levels on a genomic scale. *Genome Biol.* **2003**, *4* (9), 117.
- (4) Sanger, F. The free amino groups of insulin. *Biochem. J.* **1945**, *39* (5), 507–515.
- (5) Edman, P. Method for determination of the amino acid sequence in peptides. *Acta Chem. Scand.* **1950**, *4* (7), 283–293.
- (6) Kaiser, E.; Colescott, R. L.; Bossinger, C. D.; Cook, P. I. Color test for detection of free terminal amino groups in the solid-phase synthesis of peptides. *Anal. Biochem.* **1970**, *34* (2), 595–598.
- (7) Krause, I.; Bockhardt, A.; Neckermann, H.; Henle, T.; Klostermeyer, H. Simultaneous determination of amino acids and biogenic amines by reversed-phase high-performance liquid chromatography of the dansyl derivatives. *J. Chromatogr. A* **1995**, *715* (1), 67–79.
- (8) Udenfriend, S.; Stein, S.; Boehlen, P.; Dairman, W.; Leimgruber, W.; Weigele, M. Fluorescamine. Reagent for assay of amino acids, peptides, proteins, and primary amines in the picomole range. *Science* **1972**, *178* (4063), 871–872.
- (9) Jones, D. P.; Carlson, J. L.; Samiec, P. S.; Sternberg, P., Jr.; Mody, V. C., Jr.; Reed, R. L.; Brown, L. A. S. Glutathione measurement in human plasma evaluation of sample collection, storage and derivatization conditions for analysis of dansyl derivatives by HPLC. *Clin. Chim. Acta* **1998**, *275* (2), 175–184.
- (10) Roth, M. Fluorescence reaction for amino acids. *Anal. Chem.* **1971**, *43* (7), 880–882.
- (11) Kollipara, P. Frederick Sanger, Genomics Pioneer, Dies At 95. *Chem. Eng. News* **2013**, *91* (47), 9.
- (12) Morrison, R. T.; Boyd, R. N. *Organic Chemistry*, 3rd ed.; Allyn and Bacon: Boston, MA, 1973; p 1258.
- (13) Carey, F. A. *Organic Chemistry*, 4th ed.; McGraw Hill: New York, 2000; pp 27–28.
- (14) Sanger, F. Sequences, sequences, and sequences. *Annu. Rev. Biochem.* **1988**, *57* (1), 1–28.
- (15) Voet, D.; Voet, J. G. *Biochemistry*, 2nd ed.; Wiley: New York, 1995; p 1361.
- (16) Chambers, R. D.; Martin, P. A.; Waterhouse, J. S.; Williams, D. L. H.; Anderson, B. Mechanisms for reactions of halogenated compounds. Part 4. Activating influences of ring nitrogen and trifluoromethyl in nucleophilic aromatic substitution. *J. Fluorine Chem.* **1982**, *20* (4), 507–514.
- (17) Brown, W.; Iverson, B.; Anslyn, E.; Foote, C. *Organic Chemistry*, 7th ed.; Cengage Learning: Belmont, CA, 2013; pp 26–27.
- (18) Schnatter, W. F. K.; Rogers, D. W.; Zavitsas, A. A. Teaching Electrophilic Aromatic Substitution: Enthalpies of Hydrogenation of the Rings of C<sub>6</sub>H<sub>5</sub>X Predict Relative Reactivities; <sup>13</sup>C NMR Shifts Predict Directing Effects of X. *J. Chem. Educ.* **2015**, *92* (3), 586–588.
- (19) Pustowka, P.; Bader, H. J. Combinational synthesis of a hairy affair. Electrophilic substitution on aromatics in a different way. *Math. Naturwiss. Unterr.* **2010**, *63* (4), 216–223.
- (20) Polito, V.; Hamann, C. S.; Rhile, I. J. Carbocation Rearrangement in an Electrophilic Aromatic Substitution Discovery Laboratory. *J. Chem. Educ.* **2010**, *87* (9), 969–970.
- (21) Eby, E.; Deal, S. T. A green, guided-inquiry based electrophilic aromatic substitution for the organic chemistry laboratory. *J. Chem. Educ.* **2008**, *85* (10), 1426–1428.
- (22) Forbes, D. C.; Agarwal, M.; Ciza, J. L.; Landry, H. A. Zeroing in on electrophilic aromatic substitution. *J. Chem. Educ.* **2007**, *84* (11), 1878–1881.
- (23) Blankespoor, R. L.; Hogendoorn, S.; Pearson, A. Competitive nitration of benzene-fluorobenzene and benzene-toluene mixtures: Orientation and reactivity studies using HPLC. *J. Chem. Educ.* **2007**, *84* (4), 697–698.
- (24) Rosenthal, J.; Schuster, D. I. The anomalous reactivity of fluorobenzene in electrophilic aromatic substitution and related phenomena. *J. Chem. Educ.* **2003**, *80* (6), 679–690.
- (25) Gillis, R. G. Nucleophilic substitution in aromatic systems. *J. Chem. Educ.* **1955**, *32* (6), 296–300.
- (26) Dyal, L. K. Experiment in activated aromatic nucleophilic substitution. *J. Chem. Educ.* **1966**, *43* (12), 663–665.
- (27) Avila, W. B.; Crow, J. L.; Utermoehlen, C. M. Nucleophilic aromatic substitution: a microscale organic experiment. *J. Chem. Educ.* **1990**, *67* (4), 350–351.
- (28) Cooley, J. H. A problem-solving approach to teaching organic laboratory. *J. Chem. Educ.* **1991**, *68* (6), 503–504.
- (29) Wheeler, S. E.; Houk, K. N. Through-Space Effects of Substituents Dominate Molecular Electrostatic Potentials of Substituted Arenes. *J. Chem. Theory Comput.* **2009**, *5* (9), 2301–2312.
- (30) Weinhold, F. Natural bond orbital analysis: A critical overview of relationships to alternative bonding perspectives. *J. Comput. Chem.* **2012**, *33* (30), 2363–2379.
- (31) Shusterman, G. P.; Shusterman, A. J. Teaching chemistry with electron density models. *J. Chem. Educ.* **1997**, *74* (7), 771–776.
- (32) Sanger, M. J.; Badger, S. M., II Using computer-based visualization strategies to improve students' understanding of molecular polarity and miscibility. *J. Chem. Educ.* **2001**, *78* (10), 1412–1416.
- (33) Williamson, V. M.; Hegarty, M.; Deslongchamps, G.; Williamson, K. C.; Shultz, M. J. Identifying Student Use of Ball-and-Stick Images versus Electrostatic Potential Map Images via Eye Tracking. *J. Chem. Educ.* **2013**, *90* (2), 159–164.
- (34) Anslyn, E. V.; Dougherty, D. A. *Modern Physical Organic Chemistry*; University Science Books: Sausalito, CA, 2006; pp 14–15.
- (35) Höst, G. E.; Schönborn, K. J.; Palmerius, K. E. L. Students' Use of Three Different Visual Representations To Interpret Whether Molecules Are Polar or Nonpolar. *J. Chem. Educ.* **2012**, *89* (12), 1499–1505.

- (36) Habata, Y.; Akabori, S. Teaching  $^1\text{H}$  NMR spectrometry using computer modeling. *J. Chem. Educ.* **2001**, *78* (1), 121–123.
- (37) Sereda, G. A. A sequence of linked experiments, suitable for practical courses of inorganic, organic, computational chemistry, and NMR spectroscopy. *J. Chem. Educ.* **2006**, *83* (6), 931–933.
- (38) Sereda, G. A. Using natural bond orbitals in teaching advanced organic chemistry. *Aust. J. Educ. Chem.* **2009**, *69*, 17–22.
- (39) Hinze, S. R.; Williamson, V. M.; Deslongchamps, G.; Shultz, M. J.; Williamson, K. C.; Rapp, D. N. Textbook Treatments of Electrostatic Potential Maps in General and Organic Chemistry. *J. Chem. Educ.* **2013**, *90* (10), 1275–1281.
- (40) Kohn, W.; Becke, A. D.; Parr, R. G. Density functional theory of electronic structure. *J. Phys. Chem.* **1996**, *100* (31), 12974–12980.
- (41) Reimers, J. R.; Cai, Z. L.; Bilic, A.; Hush, N. S. The appropriateness of density-functional theory for the calculation of molecular electronics properties. *Ann. N. Y. Acad. Sci.* **2003**, *1006*, 235–251.
- (42) Frisch, M. J.; Trucks, G. W.; Schlegel, H. B.; Scuseria, G. E.; Robb, M. A.; Cheeseman, J. R.; Scalmani, G.; Barone, V.; Mennucci, B.; Petersson, G. A.; Nakatsuji, H.; Caricato, M.; Li, X.; Hratchian, H. P.; Izmaylov, A. F.; Bloino, J.; Zheng, G.; Sonnenberg, J. L.; Hada, M.; Ehara, M.; Toyota, K.; Fukuda, R.; Hasegawa, J.; Ishida, M.; Nakajima, T.; Honda, Y.; Kitao, O.; Nakai, H.; Vreven, T.; Montgomery, J. A., Jr.; Peralta, J. E.; Ogliaro, F.; Bearpark, M.; Heyd, J. J.; Brothers, E.; Kudin, K. N.; Staroverov, V. N.; Kobayashi, R.; Normand, J.; Raghavachari, K.; Rendell, A.; Burant, J. C.; Iyengar, S. S.; Tomasi, J.; Cossi, M.; Rega, N.; Millam, J. M.; Klene, M.; Knox, J. E.; Cross, J. B.; Bakken, V.; Adamo, C.; Jaramillo, J.; Gomperts, R.; Stratmann, R. E.; Yazyev, O.; Austin, A. J.; Cammi, R.; Pomelli, C.; Ochterski, J. W.; Martin, R. L.; Morokuma, K.; Zakrzewski, V. G.; Voth, G. A.; Salvador, P.; Dannenberg, J. J.; Dapprich, S.; Daniels, A. D.; Farkas, Ö.; Foresman, J. B.; Ortiz, J. V.; Cioslowski, J.; Fox, D. J. *Gaussian 09*, Revision B.01; Gaussian, Inc.: Wallingford, CT, 2010.
- (43) Dennington, R.; Keith, T.; Millam, J. *GaussView*, Version 5; Semichem Inc.: Shawnee Mission, KS, 2009.
- (44) Schmidt, M. W.; Baldridge, K. K.; Boatz, J. A.; Elbert, S. T.; Gordon, M. S.; Jensen, J. H.; Koseki, S.; Matsunaga, N.; Nguyen, K. A.; Su, S.; Windus, T. L.; Dupuis, M.; Montgomery, J. A. General atomic and molecular electronic structure system. *J. Comput. Chem.* **1993**, *14* (11), 1347–1363.
- (45) Bode, B. M.; Gordon, M. S. MacMolPlt: a graphical user interface for GAMESS. *J. Mol. Graphics Modell.* **1998**, *16* (3), 133–138.
- (46) Shusterman, A. J.; Hoistad, L. M. Teaching chemistry with electron density models. 2. Can atomic charges adequately explain electrostatic potential maps? *Chem. Educ.* **2001**, *6* (1), 36–40.
- (47) Weiner, P. K.; Langridge, R.; Blaney, J. M.; Schaefer, R.; Kollman, P. A. Electrostatic potential molecular surfaces. *Proc. Natl. Acad. Sci. U. S. A.* **1982**, *79* (12), 3754–3758.
- (48) Feldmann, R. J.; Bing, D. H.; Furie, B. C.; Furie, B. Interactive computer surface graphics approach to study of the active site of bovine trypsin. *Proc. Natl. Acad. Sci. U. S. A.* **1978**, *75* (11), 5409–5412.
- (49) Reid, S. A.; Nyambo, S.; Muzangwa, L.; Uhler, B.  $\pi$ -Stacking, C-H/ $\pi$ , and Halogen Bonding Interactions in Bromobenzene and Mixed Bromobenzene-Benzene Clusters. *J. Phys. Chem. A* **2013**, *117* (50), 13556–13563.
- (50) Gavezzotti, A. Non-conventional bonding between organic molecules. The 'halogen bond' in crystalline systems. *Mol. Phys.* **2008**, *106* (12–13), 1473–1485.
- (51) Politzer, P.; Abrahmsen, L.; Sjöberg, P. Effects of amino and nitro substituents upon the electrostatic potential of an aromatic ring. *J. Am. Chem. Soc.* **1984**, *106* (4), 855–860.
- (52) Jensen, F. *Introduction to Computational Chemistry*; John Wiley & Sons: Hoboken, NJ, 2007; pp 293–313.
- (53) Weinhold, F.; Landis, C. R. Natural bond orbitals and extensions of localized bonding concepts. *Chem. Educ. Res. Pract.* **2001**, *2* (2), 91–104.
- (54) Reed, A. E.; Weinstock, R. B.; Weinhold, F. Natural population analysis. *J. Chem. Phys.* **1985**, *83* (2), 735–746.
- (55) Suzuki, H.; Kimura, Y. Synthesis of 3,4-difluorobenzonitrile and monofluorobenzonitriles by means of halogen-exchange fluorination. *J. Fluorine Chem.* **1991**, *52* (3), 341–351.
- (56) Sun, H.; DiMaggio Stephen, G. Room-temperature nucleophilic aromatic fluorination: experimental and theoretical studies. *Angew. Chem., Int. Ed.* **2006**, *45* (17), 2720–2725.
- (57) Cieplak, A. S. Stereochemistry of nucleophilic addition to cyclohexanone. The importance of two-electron stabilizing interactions. *J. Am. Chem. Soc.* **1981**, *103* (15), 4540–4552.
- (58) Autschbach, J. Orbitals: Some Fiction and Some Facts. *J. Chem. Educ.* **2012**, *89* (8), 1032–1040.